

Received:
12 December 2017

Revised:
16 March 2018

Accepted:
20 March 2018

<https://doi.org/10.1259/bjr.20170962>

Cite this article as:

Furlan A, Almusa O, Yu RK, Sagreiya H, Borhani AA, Bae KT, et al. A radiogenomic analysis of hepatocellular carcinoma: association between fractional allelic imbalance rate index and the liver imaging reporting and data system (LI-RADS) categories and features. *Br J Radiol* 2018; **91**: 20170962.

FULL PAPER

A radiogenomic analysis of hepatocellular carcinoma: association between fractional allelic imbalance rate index and the liver imaging reporting and data system (LI-RADS) categories and features

¹ALESSANDRO FURLAN, MD, ¹OMAR ALMUSA, MD, ^{1,2}ROBINSON K YU, MD, MPH, ^{1,3}HERSH SAGREIYA, MD, ¹AMIR A BORHANI, MD, ¹KYONGTAE T BAE, MD, PhD and ^{4,5}J WALLIS MARSH, MD

¹Department of Radiology, University of Pittsburgh Medical Center, Pittsburgh, PA, United States

²Department of Radiology, Brigham and Women's Hospital, Boston, MA, USA

³Department of Radiology, Stanford University, Stanford, CA, USA

⁴Department of Surgery, West Virginia University, Morgantown, WV, USA

⁵Department of Surgery, University of Pittsburgh Medical Center, Pittsburgh, PA, USA

Address correspondence to: Dr Alessandro Furlan
E-mail: furlana@upmc.edu

Objective: To evaluate the association between the liver imaging reporting and data system (LI-RADS) categories and features and the fractional allelic imbalance (FAI) rate index of hepatocellular carcinoma (HCC).

Methods: The institutional review board approved this retrospective study. Medical records collected between January 2008 and December 2013 were reviewed to find patients with histologically confirmed HCC, FAI analysis, and CT or MR imaging of the liver. The final population included 71 patients (54 males, 17 females). Three radiologists reviewed the images using the LI-RADS v. 2014. The association between FAI and LI-RADS categories and features was tested using the Spearman's rank correlation coefficient (ρ) and the Wilcoxon rank-sum test [low FAI (<40%) vs high FAI (\geq 40%)]. A p value < 0.007 was used as the threshold for statistical significance after application of the Bonferroni correction for multiple comparisons.

Results: HCCs were classified as LR-3 ($n = 4$), LR-4 ($n = 22$), and LR-5 ($n = 45$). There was a positive correlation ($\rho = 0.264$) between FAI rate index and LI-RADS category, although not statistically significant after Bonferroni correction ($p = 0.024$). 14 of the 20 (70%) HCCs with high FAI (\geq 40%) were categorized as LR-5, 6/20 (30%) as LR-4 and none as LR-3 ($p = 0.377$). Among the evaluated LI-RADS imaging features, only lesion size showed a statistically significant different distribution in tumors with high FAI compared to those with low FAI. HCCs with FAI \geq 40% were larger (56 ± 42 mm) compared to those with FAI <40% (36 ± 30 mm; $p = 0.005$).

Conclusion: There was a positive correlation, although not statistically significant, between the LI-RADS diagnostic categories and the FAI rate of HCC. Tumors with high FAI were larger compared to those with low FAI.

Advances in knowledge: HCCs with high (\geq 40%) FAI are larger compared to those with low (<40%) FAI.

INTRODUCTION

In the era of personalized medicine, radiogenomic analysis, *i.e.* the relationship between the imaging features and the genetic expression of a disease, may provide new and tailored management for oncology patients.¹ Although hepatocellular carcinoma (HCC) represents a major health care issue in the United States,² radiogenomic analysis of this tumor has been limited.³⁻⁶

Fractional allelic imbalance (FAI) rate index is a molecular marker shown to provide excellent prognostic information on the risk of tumor recurrence in patients with

HCC undergoing liver transplantation.⁷⁻¹⁰ Nevertheless, routine utilization of FAI analysis has been limited thus far since it needs tumor tissue and, therefore, requires an invasive procedure such as a percutaneous needle biopsy. Consequently, there is an unmet need to establish imaging features associated with FAI rate either to provide a non-invasive alternative or to better select patients who would still need biopsy.

Contrast-enhanced CT and MR imaging studies are commonly performed in cirrhotic patients to diagnose HCC and to assess patients' eligibility for liver transplantation.

The liver imaging reporting and data system (LI-RADS) is a lexicon and algorithm endorsed by the American College of Radiology aimed at standardizing the interpretation of liver lesions in patients at risk for HCC.^{11,12} This system groups liver observations into five categories of risk using an algorithm, and major and ancillary imaging features as follows: LR-1, definitely benign; LR-2, probably benign; LR-3, intermediate probability of malignancy; LR-4, probably HCC; LR-5, definitely HCC. To our knowledge no study has been performed to investigate the association between the genetic expression of HCC and the LI-RADS diagnostic categories and features.

The purpose of this study was to evaluate the association between the FAI rate index of HCC and the LI-RADS categories and features.

METHODS AND MATERIALS

The institutional review board approved this retrospective, HIPAA-compliant study with waiver of informed consent.

Population

The medical record archive was interrogated to identify patients in the time interval between January 2008 and December 2013 meeting the following inclusion criteria: (1) at least one HCC proven at pathology; (2) available FAI rate of HCC in the pathology report; (3) available liver contrast-enhanced CT or MRI performed at our institution within 6 months of the pathology event date. Among the 122 available patients matching the inclusion criteria, 51 subjects were excluded because of (1) loco-regional treatment (*e.g.* transarterial chemoembolization; radiofrequency ablation) performed before imaging ($n = 24$); (2) lack of arterial phase imaging ($n = 15$); (3) radiology–pathology correlation not possible (*i.e.* multiple lesions with location not detailed on the pathology report or no lesion visible on imaging) ($n = 12$). The final study population consisted of 71 patients (54 males, 17 females; mean age 60 years; age range, 45–84 years) (Table 1).

Fractional allelic imbalance rate index

For each HCC, the FAI rate was determined as previously described (7–9). This rate is defined as the number of microsatellite markers (DNA loci) showing loss of heterozygosity (*i.e.* allelic imbalance) divided by the total number of informative markers expressed by the tumor. The nine informative microsatellite markers considered for the calculation of FAI rate index are associated with tumor-suppressor genes and were selected based on their significant correlation with recurrence-free survival.⁸

CT and MR imaging technique

40 (56%) patients underwent multidetector contrast-enhanced abdominal CT. Images were acquired before and after the intravenous injection of 100–125 ml of Optiray® 350 (ioversol – Guerbet, Villepinte, France) or Isovue® 370 (iopamidol—Bracco Diagnostics, Princeton, NJ) at a rate of 4–5 ml s⁻¹ by using a mechanical power injector. Post-contrast images were acquired during the arterial and portal venous phase. 31 (44%) subjects underwent contrast-enhanced MR. The MR imaging protocols consisted of the following sequences: pre-contrast T_1 weighted

Table 1. Characteristics of the final population

| Characteristics | Total ($n = 71$) |
|---|--------------------|
| Age in years—mean (SD) | 60 (9) |
| Gender | |
| Male | 54 (76%) |
| Female | 17 (24%) |
| Etiology of liver disease | |
| Hepatitis C | 34 (48%) |
| Hepatitis B | 3 (4%) |
| Alcohol | 7 (10%) |
| Non-alcoholic fatty liver disease | 2 (3%) |
| Primary sclerosing cholangitis | 1 (1%) |
| Multiple | 5 (7%) |
| Unknown | 19 (27%) |
| Procedure for pathological confirmation | |
| Biopsy | 10 (14%) |
| Resection | 36 (51%) |
| Explant | 25 (35%) |

dual-echo gradient-recalled-echo; axial T_2 weighted single-shot fast-spin echo; axial T_2 weighted fast-spin echo with fat saturation; axial diffusion-weighted imaging (b -values = 0 and 500 s mm⁻²; performed in 13 cases); axial 3D GRE before and after the injection of contrast as part of the multiphase dynamic study. In 23 patients, the contrast injected was Gadoxetate disodium (Eovist®, Bayer Healthcare Pharmaceuticals, Whippany, NJ), whereas 8 subjects were injected with Gadobenate dimeglumine (Multihance®; Bracco Diagnostics, Princeton, NJ). Post-contrast MR images were acquired during the arterial, portal venous, and delayed phase. A hepatobiliary phase was available in 23 cases which was obtained 20–30 min after injection of Gadoxetate disodium.

Image analysis

For each imaging study, an index lesion was identified for evaluation. When there were multiple lesions ($n = 14$), the HCC showing the highest FAI was considered for analysis. An investigator compared the pathology reports with the images and marked the location of the lesion for the readers.

Three board-certified and fellowship-trained abdominal radiologists (each with more than 3 years of experience in liver imaging), blinded to the results of the genetic analysis, independently reviewed the CT and MR imaging studies and assigned each lesion to a LI-RADS diagnostic category using the algorithm and the whole set of major and ancillary features per LI-RADS v. 2014.¹³ Tumor size was measured as the largest diameter on the axial images better showing the margins of the lesion and preferably on the post-contrast images acquired during the portal venous or delayed phase. Any disagreement among readers was resolved by consensus.

Statistical analysis

FAI rate is a continuous variable that is expressed as a percentage (0–100%). The association between LI-RADS categories, imaging features and FAI rate was initially tested calculating the Spearman's rank correlation coefficient (ρ). The following LI-RADS features were included in the analysis: size, arterial phase hyperenhancement, washout appearance, capsule appearance, presence of tumor-in-vein and mosaic architecture. Preference was given to those features recordable on both CT and MR images. We did not include growth (threshold and subthreshold) because a prior study was available only in 38 cases. We did not include the following features because of the less frequent recorded presence: corona enhancement; nodule-in-nodule; intralesional fat; lesion fat sparing; lesion iron sparing; blood products; undistorted vessels; parallels blood pool enhancement.

The 71 lesions included in the final population were then grouped into those with FAI < 40% (low FAI) and those with FAI \geq 40% (high FAI). The threshold is based on the prior literature demonstrating a significant increase in the risk of recurrence post-liver transplantation in patients with HCC showing FAI > 40%.⁹ A two-sided Wilcoxon rank-sum test was used to determine whether for each imaging feature listed above there was a significant difference in the distribution between tumors with low and high FAI. For lesion size, a receiver operating characteristic curve (ROC) and associated area-under-the-curve (AUC) were computed to obtain cut-off values for identification of tumors with FAI \geq 40%, along with relative sensitivity, specificity, positive predictive value, and negative predictive value.

A p value < 0.007 was used as the threshold for statistical significance after application of the Bonferroni correction for multiple comparisons (0.05/7). The statistical analysis was performed on Matlab (Matlab 2016b, Mathworks, Natick, MA) and on MedCalc for Windows, v. 17.1 (MedCalc Software, Ostend, Belgium).

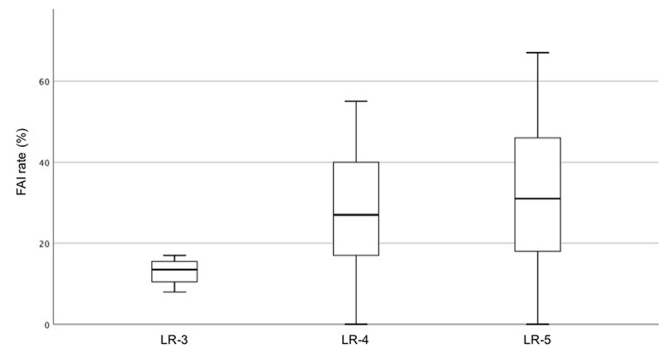
RESULTS

Our final population included 71 patients, 57 (80%) with a single HCC and 14 (20%) with multiple lesions. The median interval time from imaging to pathologic confirmation of HCC was 36 days (range, 1–173 days). The FAI rate of the index lesion ranged from 0 to 67% (mean 30%, SD 17%). Of the 71 lesions analyzed, 51 (72%) had FAI < 40% (low FAI) and 20 (28%) had FAI \geq 40% (high FAI).

The readers assigned the lesions to the following diagnostic categories: $n = 4$ (6%), LR-3 (indeterminate probability of HCC); $n = 22$ (31%), LR-4 (probably HCC); $n = 45$ (63%), LR-5 (definitely HCC). There was a positive correlation ($\rho = 0.264$) between FAI rate index and LI-RADS category, although not statistically significant after Bonferroni correction ($p = 0.024$) (Figure 1 and Table 2). 14 of the 20 (70%) HCCs with high FAI (\geq 40%) were categorized as LR-5, 6/20 (30%) as LR-4 and none as LR-3 ($p = 0.377$) (Table 3).

HCCs with high FAI were significantly larger than those with low FAI (56 ± 42 mm vs 36 ± 30 mm; $p = 0.005$) (Figure 2 and Table 3). The AUC of lesion size to discriminate between tumors

Figure 1. Box-and-whisker plot showing the distribution of FAI rate according to LI-RADS diagnostic category. LR-3 = intermediate probability of HCC; LR-4 = probably HCC; LR-5 = definitely HCC. FAI, fractional allelic imbalance; HCC, hepatocellular carcinoma.



with FAI < 40% and FAI \geq 40% was 0.72 (95% confidence interval: 0.58–0.81). The cut-off values for lesion size obtained from the ROC curve are shown in Table 4. After Bonferroni correction, no statistically significant association was found between the other LI-RADS features and the FAI rate (Table 2), and no significant difference in distribution of those features in tumors with low and high FAI was observed (Table 3). Representative examples of lesions with low and high FAI are illustrated in Figures 3 and 4.

DISCUSSION

LI-RADS represents an important step towards standardizing the interpretation of CT and MR imaging studies in patients at risk for HCC. The system assigns each liver observation to a category of malignancy risk based on a combination of major and minor imaging features.^{11,12} Although multiple studies have reported on the diagnostic accuracy and interobserver agreement of this system,^{14,15} to the best of our knowledge, ours is the first radiogenomic analysis of HCC using LI-RADS categories and features. We noticed a positive, although not statistically significant, correlation between the LI-RADS diagnostic categories and the FAI rate index ($\rho = 0.264$; $p = 0.026$). Tumors with high (\geq 40%)

Table 2. Correlation between FAI rate and LI-RADS diagnostic category and features

| | Rho | p -value |
|---------------------------------|--------|------------|
| LI-RADS diagnostic category | 0.264 | 0.026 |
| LI-RADS imaging features | | |
| Size | 0.268 | 0.024 |
| Arterial phase hyperenhancement | -0.041 | 0.732 |
| Washout appearance | 0.236 | 0.047 |
| Capsule appearance | 0.060 | 0.618 |
| Mosaic architecture | 0.217 | 0.068 |
| Tumor in vein | 0.098 | 0.443 |

FAI, fractional allelic imbalance; LI-RADS, liver imaging reporting and data system.

Spearman's rank correlation coefficient (ρ) and associated p -value.

Table 3. Distribution of LI-RADS categories and imaging features in HCC with low (<40%) and high (≥40%) FAI

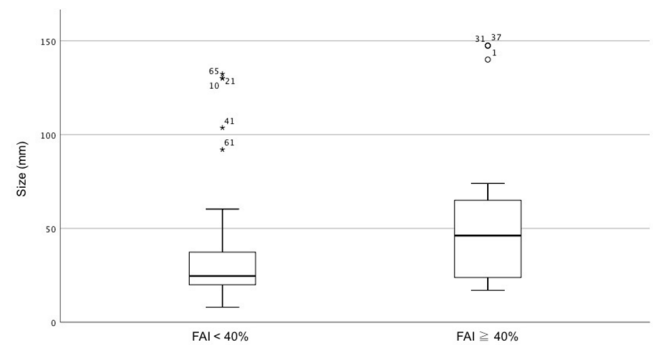
| | FAI < 40% (n = 51) | FAI ≥ 40% (n = 20) | p-value |
|-------------------------------------|-----------------------|-----------------------|---------|
| LI-RADS diagnostic category | | | |
| LR-3 | 4 (8%) | 0 (0%) | 0.377 |
| LR-4 | 16 (31%) | 6 (30%) | |
| LR-5 | 31 (61%) | 14 (70%) | |
| LI-RADS imaging features | | | |
| Size (mm) mean ± standard deviation | 36±30 | 56±42 | 0.005 |
| Arterial phase hyperenhancement | | | 0.262 |
| Present | 44 (86%) | 15 (75%) | |
| Absent | 7 (14%) | 5 (25%) | |
| Washout appearance | | | 0.429 |
| Present | 36 (71%) | 16 (80%) | |
| Absent | 15 (29%) | 4 (20%) | |
| Capsule appearance | | | 0.390 |
| Present | 21 (41%) | 6 (30%) | |
| Absent | 30 (59%) | 14 (70%) | |
| Mosaic architecture | | | 0.028 |
| Present | 16 (31%) | 12 (60%) | |
| Absent | 35 (69%) | 8 (40%) | |
| Tumor in vein | | | 0.544 |
| Present | 5 (10%) | 3 (15%) | |
| Absent | 46 (90%) | 17 (85%) | |

FAI, fractional allelic imbalance; HCC, hepatocellular carcinoma; LI-RADS, liver imaging reporting and data system.

FAI were categorized either as LR-5 (70%) or LR-4 (30%), while all HCCs categorized as LR-3 had low (<40%) FAI ($p = 0.377$).

The prognostic value of the FAI rate index has been previously shown.⁷⁻¹⁰ The FAI rate index has been used in patients with HCC to develop a system that could overcome the limitations of the currently adopted criteria for the selection of cirrhotic patients who are potential candidates for liver transplantation

Figure 2. Box-and-whisker plot showing the distribution of lesion size (i.e. maximum axial diameter) in tumors with low (<40%) and high (≥40%) FAI rate. FAI, fraction allelic imbalance.



(e.g. the Milan criteria). A study by Dvorchik et al⁹ reported that the FAI rate and neoplastic vascular invasion were the most important independent predictors of tumor-free survival after liver transplantation, with FAI rate having the highest influence. In the same study, patients with HCC showing FAI > 40% had a 14-fold increase in the risk of recurrence after liver transplantation compared to those with FAI ≤ 20%. In another study Schwartz et al¹⁰ focused on the applicability of the FAI rate index in patients beyond the Milan criteria; according to the results of this study, in patients beyond Milan criteria, an FAI score >27% and the presence of macrovascular invasion were independent predictors of tumor recurrence after liver transplantation. The post-transplant recurrence was considered as the ultimate measure of tumor aggressiveness.

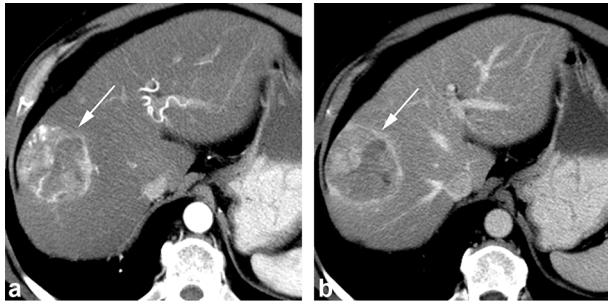
In our population, HCCs with high FAI rate index were larger (56 ± 42 mm) compared to those with low FAI (36 ± 30 mm; $p = 0.005$). The AUC of lesion size to discriminate between tumors with FAI < 40% and those with FAI ≥ 40% was 0.72. However, none of the other LI-RADS features evaluated in this study showed a statistically significant association with the FAI rate index, and the distribution of imaging features between tumors with FAI < 40% and those with FAI ≥ 40% was not statistically significant. Of note, the presence of a mosaic architecture showed a trend towards statistical significance, being recorded in 12/20 (60%) lesions with high FAI compared to 16/51 (16%) lesions with low FAI ($p = 0.028$). In the LI-RADS lexicon, a mosaic architecture indicates a heterogeneous lesion with

Table 4. Cut-off values and relative sensitivity, specificity, PPV and NPV for lesion size to identify HCC with FAI ≥ 40%

| Cut-off value (mm) | Sensitivity (%) | Specificity (%) | PPV (%) | NPV (%) |
|--------------------|-----------------|-----------------|---------|---------|
| >12 | 100 | 6 | 29 | 100 |
| >22 | 90 | 45 | 39 | 92 |
| >32 | 65 | 67 | 43 | 83 |
| >52 | 45 | 84 | 53 | 80 |
| >60 | 30 | 90 | 55 | 77 |
| >132 | 15 | 100 | 100 | 75 |

FAI, fractional allelic imbalance; HCC, hepatocellular carcinoma; NPV, negative predictive value; PPV, positive predictive value.

Figure 3. Axial contrast-enhanced CT obtained during the arterial (a) and portal venous (b) phase shows a 5.6 cm hepatocellular carcinoma diagnosed at liver resection with 50% FAI score. The lesion shows arterial phase hyperenhancement (arrow, a), washout and capsule appearance on the portal venous phase image (arrow, b) and mosaic architecture. The lesion was categorized as LR-5. FAI, fractional allelic imbalance.

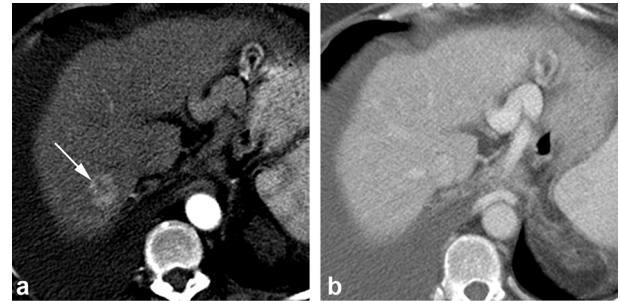


multiple internal components of different enhancement/intensity.¹³ Prior studies have shown an association between tumor heterogeneity and poorer prognosis. Kawamura et al reported that heterogeneous enhancement within HCC is associated with poorly differentiated histological grade¹⁶ and with increased tumor recurrence after radiofrequency ablation.¹⁷ More recently, Hectors et al¹⁸ showed a significant correlation between the histogram features of heterogeneity of HCC on MR imaging (e.g. standard deviation, kurtosis, skewness) and tumoral gene expression levels.

We hope that our preliminary results, despite lacking for the most part statistical significance after multiple hypothesis testing, may suggest a valid direction for future studies on the radiogenomic analysis of HCC. In our opinion, further investigation is warranted on the value of quantitative assessment of tumor heterogeneity as an adjunct to pathological data for models of predicting HCC recurrence and selecting candidates for liver transplantation.

We acknowledge several limitations of this retrospective study. Because of the strict inclusion and exclusion criteria, the final population is small. We chose to include patients with a time interval between imaging and pathology of less than 6 months and to exclude those patients with a history of loco-regional treatment because the imaging appearance may be significantly affected by treatment and tumor evolution. The lack of a significant correlation between LI-RADS features and FAI rate index

Figure 4. Axial contrast-enhanced CT obtained during the arterial (a) and portal venous (b) phase shows a 2.2 cm hepatocellular carcinoma diagnosed at explant with 27% FAI score. The lesion shows arterial phase hyperenhancement (arrow, a) and no washout or capsule appearance on the portal venous phase image. The lesion demonstrated subthreshold growth and was categorized as LR-4. FAI, fractional allelic imbalance.



may also be due to the small population size. Moreover, imaging was obtained over a long interval time (5 years) and therefore the acquisition protocols may have slightly varied. The measurement of lesion size may vary between CT and MR images, although in our opinion, the difference is attenuated by performing the measurements on the images showing the lesion margins with better clarity and favoring the post-contrast images acquired during the portal venous or delayed phase. Finally, the imaging analysis was conducted using the LI-RADS v. 2014. After the completion of our study, the newest version was released in 2017.¹⁹ Although it is difficult to assess how much the results of this study would differ when applying the newest version, we speculate no or minimal changes since a similar set of major and minor criteria is included in LI-RADS v. 2017. We acknowledge a significant update in the definition of threshold growth in LI-RADS v. 2017 compared to prior versions. In our study, this major feature was recorded in 15 cases and was key to categorize 4 lesions as LR-5 and two lesions as LR-4.

In conclusion, there was a positive correlation, although not statistically significant, between the LI-RADS diagnostic categories and the FAI rate of HCC. Tumors with high ($\geq 40\%$) FAI were larger compared to those with low ($< 40\%$) FAI.

DISCLOSURES

Alessandro Furlan has the following disclosures not related to the study: consultant for General Electric; research grant from General Electric (not related to this study); consultant for Elsevier/Amirsys.

REFERENCES

1. Rutman AM, Kuo MD. Radiogenomics: creating a link between molecular diagnostics and diagnostic imaging. *Eur J Radiol* 2009; **70**: 232–41. doi: <https://doi.org/10.1016/j.ejrad.2009.01.050>
2. El-Serag HB. Hepatocellular carcinoma: recent trends in the United States. *Gastroenterology* 2004; **127**(5 Suppl 1): S27–S34. doi: <https://doi.org/10.1053/j.gastro.2004.09.013>
3. Segal E, Sirlin CB, Ooi C, Adler AS, Gollub J, Chen X, et al. Decoding global gene expression programs in liver cancer by noninvasive imaging. *Nat Biotechnol* 2007; **25**: 675–80. doi: <https://doi.org/10.1038/nbt1306>

4. Kuo MD, Gollub J, Sirlin CB, Ooi C, Chen X. Radiogenomic analysis to identify imaging phenotypes associated with drug response gene expression programs in hepatocellular carcinoma. *J Vasc Interv Radiol* 2007; **18**: 821–30. doi: <https://doi.org/10.1016/j.jvir.2007.04.031>
5. Banerjee S, Wang DS, Kim HJ, Sirlin CB, Chan MG, Korn RL, et al. A computed tomography radiogenomic biomarker predicts microvascular invasion and clinical outcomes in hepatocellular carcinoma. *Hepatology* 2015; **62**: 792–800. doi: <https://doi.org/10.1002/hep.27877>
6. Taouli B, Hoshida Y, Kakite S, Chen X, Tan PS, Sun X, et al. Imaging-based surrogate markers of transcriptome subclasses and signatures in hepatocellular carcinoma: preliminary results. *Eur Radiol* 2017; **27**: 4472–81. doi: <https://doi.org/10.1007/s00330-017-4844-6>
7. Finkelstein SD, Marsh W, Demetris AJ, Swalsky PA, Sasatomi E, Bonham A, et al. Microdissection-based allelotyping discriminates de novo tumor from intrahepatic spread in hepatocellular carcinoma. *Hepatology* 2003; **37**: 871–9. doi: <https://doi.org/10.1053/jhep.2003.50134>
8. Marsh JW, Finkelstein SD, Demetris AJ, Swalsky PA, Sasatomi E, Bandos A, et al. Genotyping of hepatocellular carcinoma in liver transplant recipients adds predictive power for determining recurrence-free survival. *Liver Transpl* 2003; **9**: 664–71. doi: <https://doi.org/10.1053/jlts.2003.50144>
9. Dvorchik I, Schwartz M, Fiel MI, Finkelstein SD, Marsh JW. Fractional allelic imbalance could allow for the development of an equitable transplant selection policy for patients with hepatocellular carcinoma. *Liver Transpl* 2008; **14**: 443–50. doi: <https://doi.org/10.1002/lt.21393>
10. Schwartz M, Dvorchik I, Roayaie S, Fiel MI, Finkelstein S, Marsh JW, et al. Liver transplantation for hepatocellular carcinoma: extension of indications based on molecular markers. *J Hepatol* 2008; **49**: 581–8. doi: <https://doi.org/10.1016/j.jhep.2008.03.032>
11. American College of Radiology. Liver imaging reporting and data system. 2017. Available from: <https://www.acr.org/Clinical-Resources/Reporting-and-Data-Systems/LI-RADS>.
12. Santillan C, Chernyak V, Sirlin C. LI-RADS categories: concepts, definitions, and criteria. *Abdom Radiol* 2018; **43**: 101–10. doi: <https://doi.org/10.1007/s00261-017-1334-x>
13. American College of Radiology. Liver imaging reporting and data system version 2014. 2014. Available from: <https://www.acr.org/Clinical-Resources/Reporting-and-Data-Systems/LI-RADS/LI-RADS-v2014>.
14. Ronot M, Fouque O, Esvan M, Lebigot J, Aubé C, Vilgrain V. Comparison of the accuracy of AASLD and LI-RADS criteria for the non-invasive diagnosis of HCC smaller than 3 cm. *J Hepatol* 2018; **68**: 715–23. doi: <https://doi.org/10.1016/j.jhep.2017.12.014>
15. Fowler KJ, Tang A, Santillan C, Bhargavan-Chatfield M, Heiken J, Jha RC, et al. Interreader reliability of LI-RADS version 2014 algorithm and imaging features of hepatocellular carcinoma: a large international multireader study. *Radiology* 2018; **286**: 173–85. doi: <https://doi.org/10.1148/radiol.2017170376>
16. Kawamura Y, Ikeda K, Hirakawa M, Yatsuji H, Sezaki H, Hosaka T, et al. New classification of dynamic computed tomography images predictive of malignant characteristics of hepatocellular carcinoma. *Hepatol Res* 2010; **40**: 1006–14. doi: <https://doi.org/10.1111/j.1872-034X.2010.00703.x>
17. Kawamura Y, Ikeda K, Seko Y, Hosaka T, Kobayashi M, Saitoh S, et al. Heterogeneous type 4 enhancement of hepatocellular carcinoma on dynamic CT is associated with tumor recurrence after radiofrequency ablation. *AJR Am J Roentgenol* 2011; **197**: W665–W673. doi: <https://doi.org/10.2214/AJR.11.6843>
18. Hectors SJ, Wagner M, Bane O, Besa C, Lewis S, Remark R, et al. Quantification of hepatocellular carcinoma heterogeneity with multiparametric magnetic resonance imaging. *Sci Rep* 2017; **7**: 2452. doi: <https://doi.org/10.1038/s41598-017-02706-z>
19. Elsayes KM, Hooker JC, Agrons MM, Kielar AZ, Tang A, Fowler KJ, et al. 2017 version of LI-RADS for CT and MR imaging: an update. *Radiographics* 2017; **37**: 1994–2017. doi: <https://doi.org/10.1148/rg.2017170098>